

Separation of *p*-Divinylbenzene by Selective Room-Temperature Adsorption Inside Mg-CUK-1 Prepared by Aqueous Microwave Synthesis**

Beau Saccoccia, Alisha M. Bohnsack, Nolan W. Waggoner, Kyung Ho Cho, Ji Sun Lee, Do-Young Hong, Vincent M. Lynch, Jong-San Chang,* and Simon M. Humphrey*

Abstract: A new Mg^{II}-based version of the porous coordination polymer CUK-1 with one-dimensional pore structure was prepared by microwave synthesis in water. Mg-CUK-1 is moisture-stable, thermally stable up to 500°C, and shows unusual reversible soft-crystal behavior: dehydrated single crystals of the material selectively adsorb a range of organic molecules at ambient temperature and pressure. Both polar and apolar aromatic compounds, including pyridine, benzene, *p*-xylene, and *p*-divinylbenzene (*p*-DVB), are all readily adsorbed, while other isomers from complex mixtures of xylenes or DVBs are selectively excluded. The solvent-loaded structures have been studied by single-crystal X-ray diffraction. Time-dependent liquid sorption experiments using commercially available DVB demonstrate a high and rapid selective adsorption of *p*-DVB and exclusion of *m*-DVB and ethylvinylbenzene isomers.

A number of porous coordination polymers (PCPs) have been shown to possess the ability to effectively separate complex mixtures of gases^[1] and, less commonly, of liquid hydrocarbons.^[2] The latter represents a tangible application for such materials, especially to achieve separations that cannot be easily performed using common large-scale separation methods (e.g., column chromatography, ion exchange,

fractional distillation).^[3,4] One such example concerns the separation of isomers of divinylbenzene (DVB): *p*-DVB is important in the manufacture of cross-linked styrene polymers, which, paradoxically, are utilized in the manufacturing of ion-exchange resins.^[4] DVB is prepared by dehydrogenation of crude mixtures of *o*-, *m*-, and *p*-diethylbenzene. Commercially available DVB consists of approximately 80% *m*- and *p*-DVB along with the products of partial dehydrogenation, *m*- and *p*-ethylvinylbenzene (EVB). From an industrial standpoint, pure *p*-DVB is most preferred for the formation of ordered cross-linked styrene/*p*-DVB copolymers, but large-scale separation approaches have proven to be inefficient.^[5]

In 2007, we published the discovery of a highly porous cobalt(II)-based coordination polymer named CUK-1, which has received significant attention because of its exceptional ability to separate complex gas mixtures.^[6] CUK-1 is based on 2,4-pyridinedicarboxylic acid (2,4-pdc) and contains one-dimensional channels with square pore windows. The material was shown to be highly robust, owing to the presence of infinite one-dimensional metal hydroxide chains that support a corrugated wall structure. One potential drawback of transition-metal-based materials is the potential for slow hydrolytic decomposition. Ongoing efforts to determine methods for the preparation of more highly stable phases of CUK-1 using alternative metals have ultimately yielded a fast, reproducible, and high-yielding method for the production of a Mg^{II} analogue. Mg-CUK-1 is conveniently prepared in water with a rapid and energy-efficient microwave(μ w)-assisted method that yields a crystalline product in only 35 min at 200°C.

Replacement of Co^{II} with Mg^{II} was our ultimate goal, because the resulting Mg-CUK-1 is significantly (19.2%) lighter than the original material, and is thermally and chemically more stable because of the higher hardness of Mg^{II}. Mg^{II} is also cheaper and comparatively nontoxic compared to most transition metals, making it an ideal choice for scale-up purposes. The Mg analogue can also be prepared using a conventional (cv) heating method at 220°C in H₂O for 15 h. Although the average crystallite size obtained from cv heating is significantly larger, the reaction yield and (more importantly) the bulk textural properties are both superior for μ w-synthesized materials (see below).

The Mg^{II} centers in Mg-CUK-1 are octahedrally coordinated and bridge into infinite chains of edge- and vertex-sharing Mg₃OH triangles. The lattice connectivity of Mg-CUK-1 is identical to that of Co-CUK-1, but the space group of the as-synthesized material is different (*P*2₁/*c* versus *C*2/*c*).

[*] B. Saccoccia, A. M. Bohnsack, N. W. Waggoner, Dr. V. M. Lynch, Prof. S. M. Humphrey
Department of Chemistry, The University of Texas at Austin
Welch Hall 2.204, 105 E. 24th St. Stop A5300
Austin, TX 78712-1224 (USA)
E-mail: smh@cm.utexas.edu

K. H. Cho, J. S. Lee, Dr. D.-Y. Hong, Dr. J.-S. Chang
Catalysis Center for Molecular Engineering
Korea Research Institute of Chemical Technology
P.O. Box 107, Yusong, Daejeon 305-600 (Korea)
E-mail: jschang@kRICT.re.kr

Dr. J.-S. Chang
Department of Chemistry, Sungkyunkwan University (Korea)

[**] We gratefully acknowledge Prof. Bradley J. Holiday and Minh Nguyen (U.T. Austin) for DFT results, Dr. Young Kyu Hwang (KRICT) for helpful discussions, and the Welch Foundation (F-1738), the DRC Program (SK-1421) supported by NRCST, and the Center for Hybrid Interface Materials (HIM) for the Global Frontier R&D Program (2013-073298), funded by the Ministry of Science, ICT & Future Planning, and the Institutional Collaboration Program between KRICT and KIMM supported by NRCST, for funding this work.

Supporting information for this article is available on the WWW under <http://dx.doi.org/10.1002/anie.201411862>.

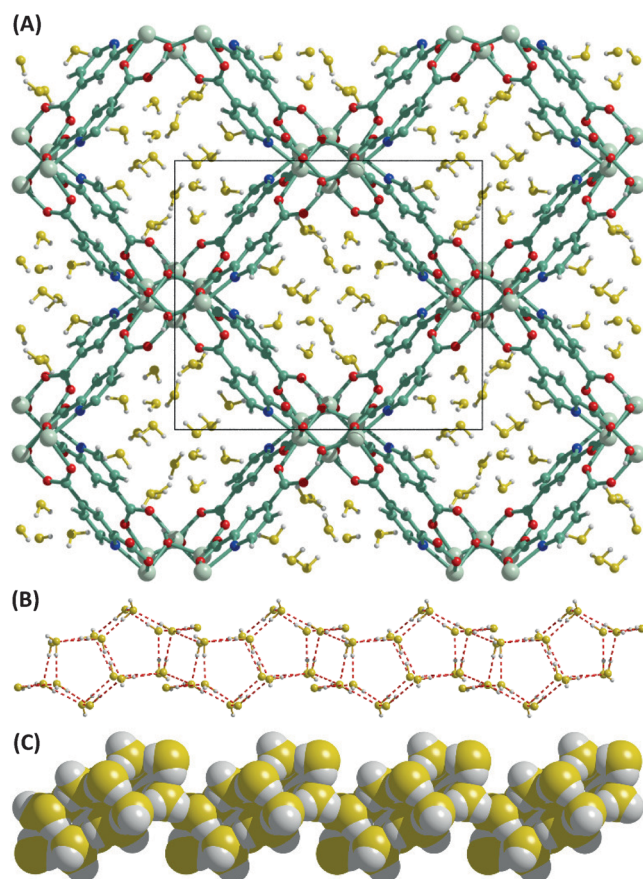


Figure 1. A) Structure of as-synthesized Mg-CUK-1 viewed down the crystallographic *a*-axis; solvent O atoms are drawn in yellow for clarity. B) A single chain of H-bonded H₂O molecules that form pentameric drums. C) Space-filling view of a single H₂O chain, depicting the “lumpy” channel topology.

The lower symmetry of the new material can be explained with the positions of guest H₂O molecules inside the channels (Figure 1 A; yellow). A network of close-range H-bonding interactions that include μ_3 -OH moieties resident in the pore walls results in the formation of a remarkably well-ordered pseudo-ice phase at room temperature; the solvent is so well ordered that all H atoms were directly located in the peak-difference map. Full resolution of the H₂O structure revealed infinite chains of (H₂O)₁₆ cages comprised of face-sharing pentameric drums (Figure 1 B,C). H···O contact distances lie in the range 2.71–2.96 Å compared with 2.76 Å in the Ih-ice phase.^[7] A space-filling view of the one-dimensional “ice” chains provides a perspective of the channel topology in Mg-CUK-1, which takes the form of undulating channels that contain pockets linked by smaller apertures (Figure 1 C).

Despite the extended H-bonding network, Mg-CUK-1 is surprisingly easily dehydrated by gentle heating (50 °C) under vacuum over 1 h, or alternatively at ambient pressure using a stream of heated (70–100 °C) N₂ gas. Thermogravimetric analysis (TGA) confirmed a rapid mass loss of 22 wt % between 20 and 50 °C, after which there is a very large window of stability until the onset of polymer degradation at about 500 °C (Figure S5 and S6 in the Supporting Information). Heating a single crystal in a stream of dry N₂ and subsequent

in situ X-ray diffraction analysis at 100 °C revealed complete dehydration accompanied by retention of the three-dimensional order. Notably, the symmetry spontaneously changes to *C2/c* upon dehydration. In comparison to the as-synthesized structure, dehydrated crystals show a concertina distortion perpendicular to the direction of channel propagation (so-called soft-crystal behavior),^[8] resulting in diamondoid-shaped channels (Figure S11). Cooling of a dehydrated crystal to –143 °C under dry N₂ did not result in further structural deformation (or reversion to the original primitive space group), which indicates that the concertinaing is simply due to loss of H₂O from the pores and is not a temperature-dependent phase transition of the PCP.

Dehydrated Mg-CUK-1 is stable when stored in air and when re-suspended in fresh H₂O, as confirmed by bulk powder X-ray diffraction analysis (PXRD; Figure S1 and S4). The bulk textural properties of the material were assessed as a function of the synthetic method, using a number of small-molecule probe gases in the range 0–1 atm (Figure S8 and S9). Regardless of the heating method, Mg-CUK-1 showed an adsorption preference of CO₂ over H₂, N₂, and CH₄. H₂ and CH₄ were more strongly adsorbed than N₂, as was originally observed for the Co^{II}-based analogue.^[6] The total sorption capacities and estimated CO₂ BET surface area of μ w-Mg-CUK-1 were found to be higher than for cv-Mg-CUK-1 for all gases studied (Table 1). Fast crystallization under μ w heating

Table 1: Summary of gas adsorption properties of Mg-CUK-1 as a function of the synthetic method.

Synthetic method	V_{N_2} [m ² g ^{−1}]	V_{N_2} [cm ³ g ^{−1}]	V_{CO_2} [cm ³ g ^{−1}]	V_{H_2} [cm ³ g ^{−1}]	V_{CH_4} [cm ³ g ^{−1}]
μ w	602	68	196	143	95
cv	521	32	165	60	84

results in smaller crystallites, which should have more accessible pore openings and shorter channels that could be more efficiently filled by guest adsorbates. Scanning electron microscopy (SEM) analysis of the as-synthesized materials revealed average crystallite sizes of 150 × 250 and 10 × 30 μ m for the cv- and μ w-prepared samples, respectively (Figure S7). Interestingly, the measured CO₂ BET surface area of cv-Mg-CUK-1 was increased by 12 % by simple mechanical grinding of the crystallites to an average size resembling that of the as-synthesized μ w-material (Figure S10). While the average particle size is obviously an important factor, it is plausible that other effects such as pore blocking by unreacted organic and inorganic components may also differ between the synthetic routes, or that the μ w route provides Mg-CUK-1 with fewer framework defects.

We then explored the potential use of μ w-Mg-CUK-1 for the selective adsorption/extraction of a range of aromatic molecules from the liquid phase. In all experiments, dehydrated crystallites were suspended in the water-free solvents over 1–5 days at room temperature. The individual crystals retained their crystallinity during the adsorption process, and remarkably allowed for the collection of new single-crystal X-ray structures with completely resolved, ordered solvent

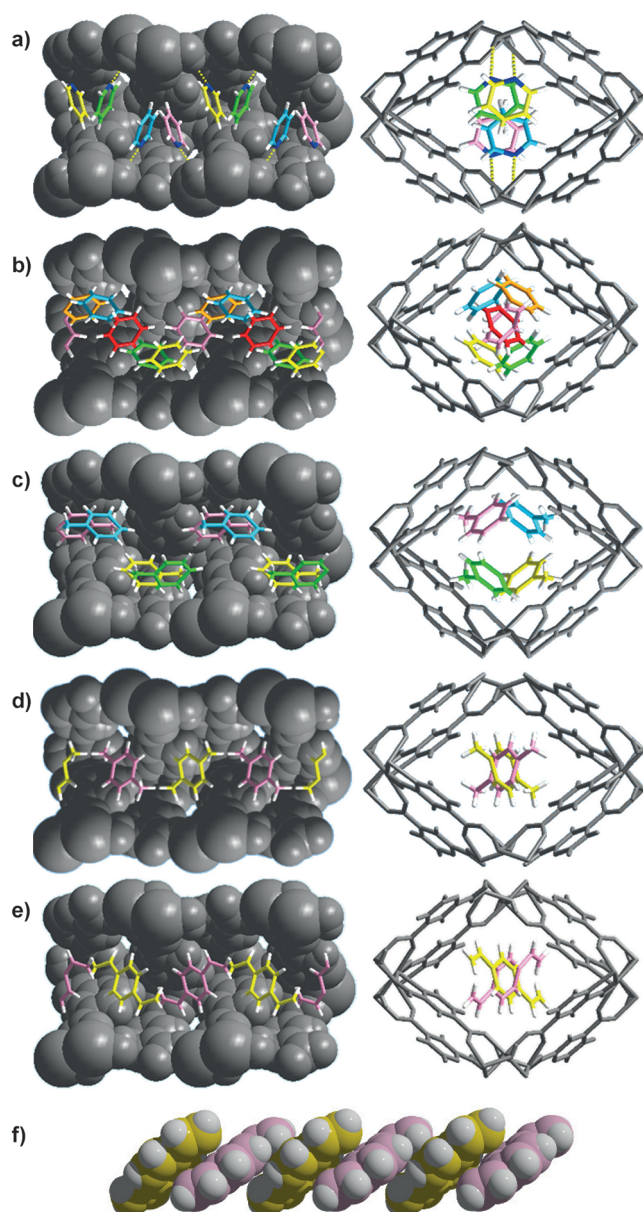


Figure 2. Crystal structures of solvent-loaded Mg-CUK-1. The polymer is drawn in grey and all crystallographically unique solvent positions are shown in different colors. a) Pyridine, b) benzene, c) toluene, d) *p*-xylene, e) *p*-DVB adsorbed from a crude mixture, f) packing arrangement of a single chain of *p*-DVB monomers.

molecules located inside the channels (Figure 2 and S2). The sorption capacity of Mg-CUK-1 differs from solvent to solvent, as might be expected based on packing densities and the presence of favorable host–guest and guest–guest interactions (see below). The absolute adsorption capacities were assessed by comparing the model solvent occupancies obtained from the single-crystal studies to bulk samples of solvent-loaded crystals, analyzed by ^1H NMR spectroscopy upon digestion in acidic $[\text{D}_6]\text{acetone}/\text{D}_2\text{O}$, and by TGA analysis (see Table S3).

Adsorption of pyridine inside dehydrated Mg-CUK-1 resulted in a zigzag packing arrangement directed by short-range (2.52 \AA) donor–acceptor contacts between pyr-

idine N and hydroxide H atoms in the channel walls (Figure 2a). Benzyl alcohol showed a similar behavior (Figure S15). In contrast, apolar benzene becomes arranged in an undulating ribbon with six unique (and partially occupied) orientations based on a combination of face-to-face host–guest π – π interactions (centroid–centroid = 4.31 \AA) and T-shaped benzene H to channel wall (2,4-pdc)– π interactions (4.05 \AA ; Figure 2b and S12A).^[9] Toluene formed a simpler ordered phase, with similar π – π interactions (centroid–centroid = 4.30 \AA ; Figure 2c and S16B).

The adsorption of xylene isomers was then studied. A handful of PCPs have been shown to selectively separate xylene isomers.^[10] Interestingly, in this case an ordered crystalline phase was obtained only for *p*-xylene-treated Mg-CUK-1 (Figure 2d); single crystals treated with *o*- and *m*-xylene remained highly crystalline, but electron density corresponding to less than one electron per site was smeared throughout the centers of the channel voids. TGA and elemental microanalysis of the materials indicated at least some adsorption for all isomers (see the Supporting Information). Liquid (vapor) sorption isotherms collected using each pure isomer in the range $p/p_0 = 0$ – 0.7 at 50°C provide more valuable insight (Figure 3). It is apparent that dehydrated Mg-

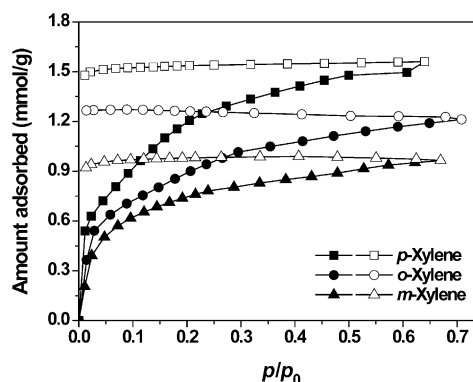


Figure 3. Adsorption–desorption profiles for vapors of the three xylene isomers in dehydrated Mg-CUK-1 recorded at 50°C . In the graph, closed and open symbols display adsorption and desorption data, respectively.

CUK-1 can adsorb each isomer, but the relative capacity is of the order $p > o > m$. The minimum guest-accessible dimension of the pore openings in dehydrated Mg-CUK-1 is 8.0 \AA (obtained directly from the crystal structure; Figure S11); the critical diameters of the three xylene isomers (*o*: 6.6 \AA , *m*: 6.4 \AA , *p*: 5.7 \AA ; Figure S12) should therefore permit easy access of each isomer to the interior of the channels. Notably, the crystal structure of the *p*-xylene-loaded material shows that guest–guest interactions are the dominant sorption force; however, close-range host–guest interactions that were dominant for smaller aromatic compounds were not evident. Instead, head-to-tail-type intermolecular CH_3 – π guest–guest interactions are prevalent (centroid–C = 4.24 \AA ; Figure S16C).^[9] The strong hysteresis observed in the desorption isotherms (open symbols; Figure 3) is also strong evidence for the presence of favorable guest–guest π – π interactions; similar

behavior has been observed in other micro- and mesoporous materials.^[11] Furthermore, when activated Mg-CUK-1 was exposed to a 1:1:1 mixture of the three xylene isomers, single-crystal analysis revealed a *p*-xylene-loaded structure with an identical packing arrangement as obtained when pure *p*-xylene was the adsorbate. This indicated to us that Mg-CUK-1 might have the ability to selectively adsorb other *p*-substituted aromatic molecules from mixtures of isomers, based on their preferential packing linearly within the undulating one-dimensional channels.

Pure fractions of DVB isomers are not easily obtained, due to the inherent purification issues outlined above. Instead, we directly treated a sample of dehydrated Mg-CUK-1 with a commercially available technical-grade DVB, which contained $\geq 79\%$ of a mixture of *m*- and *p*-DVB along with $\leq 21\%$ of *m*- and *p*-EVB, naphthalene, and 4-*tert*-butylcatechol as stabilizer. Strikingly, after standing for three days, single crystals were found to contain only *p*-DVB (Figure 2e). The packing arrangement of *p*-DVB is very similar to that of *p*-xylene; guest-guest packing interactions are clearly dominant. Individual *p*-DVB monomers are planar and tightly packed into the one-dimensional chains with very close-range (3.63 \AA) π -vinylene interactions (Figure 2f and S12D). Kitagawa and co-workers previously studied selective DVB adsorption and subsequent in situ polymerization by a terephthalate-based PCP with one-dimensional channels.^[12] They found that smaller channels selectively gave *p*-substituted polymers and it was concluded that the packing orientation of the monomers inside the pores affected the extent of polymerization: a face-to-face orientation of the monomers was thought to promote polymerization, but single-crystal structures of the loaded materials were not obtained. This study suggests that *p*-DVB is selectively adsorbed inside the one-dimensional channels because a head-to-tail orientation results in the most favorable adsorption enthalpy (the critical diameters of all DVB and EVB isomers are similar to those of the corresponding xylene isomers, so it is possible for all molecules to enter the channels; Figure S12).

To further investigate the potential usefulness of Mg-CUK-1 as a medium for the separation of DVB isomers, larger quantities (ca. 1 g) of Mg-CUK-1 were employed to facilitate a time-dependent separation study. SEM imaging confirmed that the crystallites are very robust and retain their bulk structure upon loading (Figure S14). Commercially available DVB is notoriously difficult to handle at elevated temperatures because it tends to oligomerize. As the DVB isomers also have low vapor pressures, it is difficult to record useful vapor sorption isotherms. However, 1,4-dibromonaphthalene can be used as a convenient GC-MS internal standard to allow for the accurate analysis of relative isomer amounts in liquid sorption studies. In direct support of the above single-crystal observations, liquid sorption results using bulk samples of Mg-CUK-1 treated with a crude DVB mixture at 25°C confirmed a very high sorption affinity of *p*-DVB over the three other major components, while *m*-DVB itself became enriched in the supernatant liquid (Figure 4). The adsorption selectivity for *p*-DVB in Mg-CUK-1 is considerable after only 3 h exposure time, with a selectivity factor of

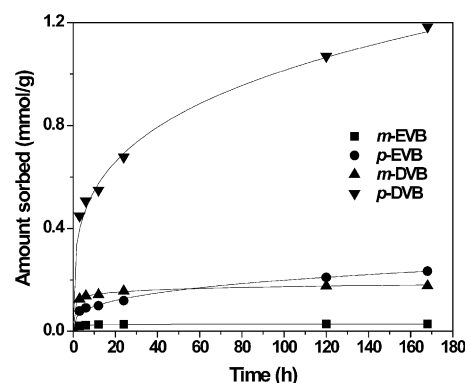


Figure 4. Liquid sorption profiles for the DVB mixture in dehydrated Mg-CUK-1 recorded at 25°C as a function of sorption time.

8.2. This value gradually increased with time up to 7 days, reaching a selectivity factor of 15.0 (1.18 mmol g^{-1} corresponds to $0.154 \text{ g p-DVB per g Mg-CUK-1}$).

There are two plausible explanations for the impressive selective adsorption observed: a) it is clear that the *p*-DVB monomers are most rapidly adsorbed into the channels, possibly because the inherent π conjugation and extended resonance in the *p*-DVB isomer maintains a planar structure that can more easily enter the channels; b) the resulting *p*-isomer-loaded structure is most stable because of the favorable resulting host-guest and guest-guest stacking forces. Head-to-tail *m*-DVB stacking is more difficult because of the substitution pattern. Ab initio DFT calculations of *m*- and *p*-DVB also suggest that fully planar conformations are energetically most favored in the gas phase (see the Supporting Information). Meanwhile, the partially saturated EVB isomers would be unable to establish head-to-tail π -vinylene interactions that are necessary to promote ordered packing inside the channels, hence the very low uptake of these. A comparison of the theoretical void space in Mg-CUK-1 to the actual volume required per adsorbed molecule reveals that the pores are more fully occupied by smaller molecules such as pyridine, which can pack more efficiently and engage in host-guest H-bonding interactions; meanwhile, the total space occupied by other, larger adsorbates was in the range 72–89% (based on TGA loading data; Table S4).

In conclusion, Mg-CUK-1 is a remarkably stable porous material that can be prepared in large quantities using a convenient and environmentally benign microwave-assisted aqueous method. The structural robustness of Mg-CUK-1 has enabled a detailed structural investigation of hydrocarbon adsorption, which provides a clear explanation for its ability to selectively adsorb *p*-isomers of xylene and DVB from complex mixtures of isomers.

Experimental Section

Synthesis of $\mu\text{w-Mg-CUK-1}$: 2,4-Pyridinedicarboxylic acid (170 mg, 1.0 mmol) and KOH (2.0 M, 2.0 cm^3) in H_2O (2.0 cm^3) were added to a stirred solution of $\text{Mg}(\text{NO}_3)_2\cdot\text{hydrate}$ (380 mg, 1.5 mmol) in H_2O (3.0 cm^3) to give a viscous, opaque slurry, which was heated to 200°C for 35 min in a MARS microwave (CEM Corp.) inside 100 cm^3

Teflon-lined Easy-Prep reaction vessels. The reaction temperature was monitored using a fiber-optic sensor. After cooling (30 min), the crystalline solid was purified by brief (3×20 s) cycles of sonication in fresh H_2O (20 cm^3), followed by decanting of the cloudy supernatant. Large, colorless prismatic crystals were isolated (average yield: 124 mg). C,H,N analysis (%) calcd for $\text{C}_{14}\text{H}_8\text{Mg}_3\text{N}_2\text{O}_{10} \cdot 9\text{H}_2\text{O}$: C 28.1, H 4.38, N 4.68; found: C 28.2, H 4.06, N 4.99.

Synthesis of cv-Mg-CUK-1: The method described above was used to prepare the reaction slurry, which was then transferred to a 23 cm^3 Teflon-lined autoclave (Parr Corp.), heated at 210°C for 15 h, cooled for 6 h, and purified as described above (average yield: 58 mg).

Dehydration and solvent loading: Bulk samples of Mg-CUK-1 purified as described above were evaporated to dryness in air, then dried further under vacuum at $50\text{--}60^\circ\text{C}$ for at least 2 h. C,H,N analysis (%) calcd for $\text{C}_{14}\text{H}_8\text{Mg}_3\text{N}_2\text{O}_{10}$: C 38.6, H 1.85, N 6.42; found: C 38.4, H 2.03, N 6.39. Longer evacuation times did not result in any sample degradation. Small quantities (5–10 mg) of dehydrated material were transferred to scintillation vials under nitrogen and covered with the pre-dried solvent. The crystals were left to stand for two days before analysis. See the Supporting Information for further characterizing data.

Sorption of aromatic hydrocarbons: Vapor-phase adsorption experiments with xylene isomers were carried out at 50°C using an Intelligent Gravimetric Analyzer (IGA, Hiden Analytical Ltd.). Liquid sorption experiments of technical-grade DVB using 1,4-dibromonaphthalene as internal standard were performed in a sample vial (10 mL) at 25°C . Detailed procedures of these experiments are provided in the Supporting Information.

Keywords: divinylbenzene · isomer separation · liquid sorption · metal–organic frameworks · porous coordination polymers

How to cite: *Angew. Chem. Int. Ed.* **2015**, *54*, 5394–5398
Angew. Chem. **2015**, *127*, 5484–5488

- [1] a) A. J.-R. Li, R. J. Kuppler, H.-C. Zhou, *Chem. Soc. Rev.* **2009**, *38*, 1477–1504; b) B. U. Mueller, M. Schubert, F. Teich, H. Puetter, K. Schierle-Arndt, J. Pastre, *J. Mater. Chem.* **2006**, *16*, 626–636; c) J.-R. Li, J. Sculley, H.-C. Zhou, *Chem. Rev.* **2012**, *112*, 869–932.
[2] See for example: a) C.-X. Yang, X.-P. Yan, *Anal. Chem.* **2011**, *83*, 7144–7150; b) H. Wu, Q. Gong, D. H. Olson, J. Li, *Chem. Rev.* **2012**, *112*, 836–868; c) J.-Y. Cheng, P. Wang, J.-P. Ma, Q.-K. Liu, Y.-B. Dong, *Chem. Commun.* **2014**, *50*, 13672–13675; d) E. D.

- Bloch, W. L. Queen, R. Kirshna, J. M. Zadronzy, C. M. Brown, J. R. Long, *Science* **2012**, *335*, 1606–1610; e) S. Han, Y. Wei, C. Valentine, I. Lagzi, J. J. Gassensmith, A. Coskun, J. F. Stoddart, B. A. Grzybowski, *J. Am. Chem. Soc.* **2010**, *132*, 16358–16361.
[3] R. El Osta, A. Carlin-Sinclair, N. Guillou, R. I. Walton, F. Vermoortele, M. Maes, D. de Vos, F. Millange, *Chem. Mater.* **2012**, *24*, 2781–2791.
[4] A. A. Zagorodni, *Ion Exchange Materials: Properties and Applications*, Elsevier, **2006**.
[5] R. H. Wiley, G. DeVenuto, T. K. Venkatachalam, *J. Gas. Chromatog.* **1967**, *5*, 590–591.
[6] a) S. M. Humphrey, J.-S. Chang, S. H. Jung, J. W. Yoon, P. T. Wood, *Angew. Chem. Int. Ed.* **2007**, *46*, 272–275; b) *Angew. Chem.* **2007**, *119*, 276–279; c) J. W. Yoon, S. H. Jung, Y. K. Hwang, S. M. Humphrey, P. T. Wood, J.-S. Chang, *Adv. Mater.* **2007**, *19*, 1830–1834.
[7] W. F. Kuhs, M. S. Lehmann, *Water Science Reviews*, Vol. 2, Oxford University Press, Oxford, **1986**, pp. 1–66.
[8] Y. Hijikata, S. Horike, D. Tanaka, J. Groll, M. Mizuno, J. Kim, M. Takata, S. Kitagawa, *Chem. Commun.* **2011**, *47*, 7632–7634.
[9] C. R. Martinez, B. Iverson, *Chem. Sci.* **2012**, *3*, 2191–2201.
[10] a) A. Kasik, Y. S. Lin, *Sep. Purif. Technol.* **2014**, *121*, 38–45; b) D. Peralta, K. Barthelet, J. Pérez-Pellitero, C. Chizallet, G. Chaplais, A. Simon-Masseron, G. D. Pirngruber, *J. Phys. Chem. C* **2012**, *116*, 21844–21855; c) Z.-Y. Gu, X.-P. Yan, *Angew. Chem. Int. Ed.* **2010**, *49*, 1477–1480; *Angew. Chem.* **2010**, *122*, 1519–1522; d) T. Remy, G. V. Baron, J. F. M. Denayer, *Langmuir* **2011**, *27*, 13064–13071; e) L. Alaerts, C. E. A. Kirschhock, M. Maes, M. A. van der Veen, V. Finsy, A. Delpa, J. A. Martens, G. V. Baron, P. A. Jacobs, J. E. M. Denayer, D. E. De Vos, *Angew. Chem. Int. Ed.* **2007**, *46*, 4293–4297; *Angew. Chem.* **2007**, *119*, 4371–4375.
[11] a) V. R. Choudhary, K. Mantri, *Microporous Mesoporous Mater.* **2000**, *40*, 127–133; b) R. Wendelbo, R. Roque-Malherbe, *Microporous Mater.* **1997**, *10*, 231–246; c) W. Makowski, M. Mańko, P. Zabierowski, K. Mlekodaj, D. Majda, J. Szklarzewicz, W. Łasocha, *Thermochim. Acta* **2014**, *587*, 1–10; d) K. Yang, Q. Sun, F. Xue, D. Lin, *J. Hazard. Mater.* **2011**, *195*, 124–131.
[12] T. Uemura, D. Hiramatsu, Y. Kubota, M. Takata, S. Kitagawa, *Angew. Chem. Int. Ed.* **2007**, *46*, 4987–4990; *Angew. Chem.* **2007**, *119*, 5075–5078.

Received: December 9, 2014

Revised: January 25, 2015

Published online: March 3, 2015